



## **SEISMIC DAMAGE MITIGATION OF REINFORCED CONCRETE BRIDGE PIERS BY UNBONDING LONGITUDINAL REINFORCEMENTS**

**Govinda Raj PANDEY<sup>1</sup>, Hiroshi MUTSUYOSHI<sup>2</sup>**

### **SUMMARY**

The recent major earthquakes such as Hyogo-ken Nanbu earthquake in 1995 (hereafter Kobe Earthquake) showed that most of the fatal collapses of RC structures were caused by shear failure. Design codes in Japan, subsequently revised, demand a large quantity of shear reinforcement to prevent shear failure and to maintain sufficient ductility. The resulting design comprises of the shear reinforcements with a very high volumetric ratio, which creates negative impact both in terms of constructability and economy. In an attempt to find some alternative methods to handle this issue without the conventional reliance on shear reinforcements alone, an investigation was carried out to examine the enhancement of seismic performance of reinforced concrete columns such as shear strength and ductility by controlling bond of longitudinal reinforcements. Six 300 x 300 mm square RC columns were tested under reversed cyclic loading. Three different bond conditions varying from the perfect bond with the use of ordinary deformed bars to the perfect unbond by completely eliminating bond between steel and concrete were employed in the experiment. A poor bond condition was achieved by replacing deformed bars by round bars with a coat of grease applied on the surface. Test results showed that this method is very effective in completely altering the failure mode at the ultimate state from shear to flexure. This method was also found to produce remarkable improvement in the ductility of RC columns. In order to further study the behavior of unbonded column under earthquake loading, seismic response analysis was carried out. The results revealed that the unbonded columns show larger seismic displacement than that of ordinary RC column due to smaller amount of energy absorption.

### **INTRODUCTION**

Despite numerous researches on shear behavior, which have been intensively carried out since past several decades [1,2], to construct a structure avoiding undesirable shear collapse still poses a great challenge. The recent strong earthquakes, such as Kobe Earthquake in Japan, have further demonstrated several catastrophic shear failure of RC bridge piers [3,4]. Investigation on the bridges damaged by earthquake shows that shear failure mainly occurs due to the inadequacy of web reinforcements apart from the deficient reinforcement detailing [5]. After Kobe Earthquake, highway bridge design code of Japan was subjected to a major modification. In the new design code, the design seismic load has been increased to a great extent and design is carried out so that the structure can maintain required

---

<sup>1</sup> Graduate Student, Saitama University, Japan. Email:govinda@mtr.civil.saitama-u.ac.jp

<sup>2</sup> Professor, Saitama University, Japan. Email: mutuyosi@mtr.civil.saitama-u.ac.jp

performance after an earthquake [6]. RC members designed by the current code require a large amount of shear reinforcements. Large quantities of reinforcements, however, make the detailing of the member complicated and the congestion leads to the difficulty in placing concrete. It therefore becomes counterproductive both in terms of constructability and economy. This underscores the need to investigate some alternative ways of shear capacity improvement without the heavy reliance on shear reinforcements alone.

Elimination of the bond between longitudinal bar and concrete leads to major change in stress distribution inside the concrete [7]. With no flexural cracks in unbonded shear span, it is apparent that the concrete body mainly remains under diagonal compression with straight thrust line resembling a tied arch mechanism. Thus, this stress condition makes the whole shear span to be free of cracks and is effective in preventing diagonal shear failure, which can eventually enhance the shear performance of columns [8-12]. The main purposes of this study are to investigate the possible enhancement of seismic performance of RC columns by controlling bond of longitudinal reinforcement and to analyze seismic response behavior of RC columns with unbonded reinforcement.

## EXPERIMENTAL PROGRAM

In order to investigate the influence of unbonding longitudinal reinforcement on seismic behavior of RC columns, six specimens were tested under reversed cyclic loading.

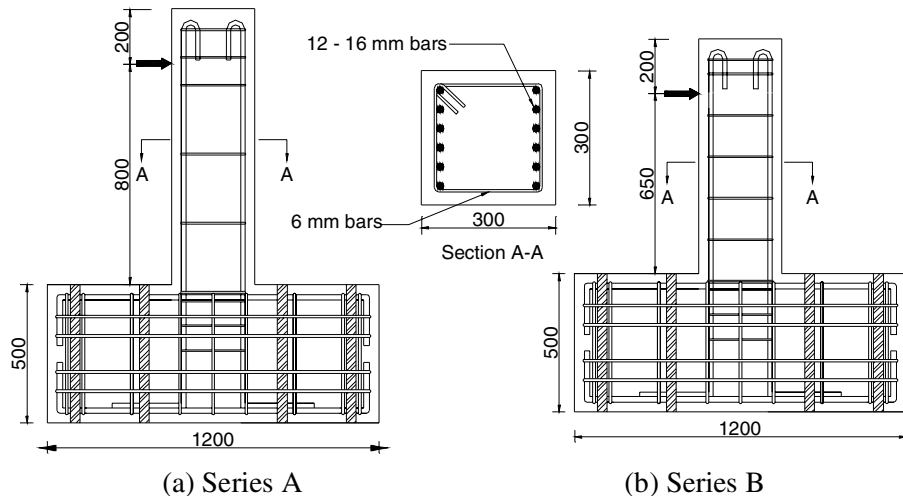


**Fig. 1: Details of test Specimen**

### Specimen Details

Specimens were divided into two series depending on their shear-span-to-depth ( $a/d$ ) ratio. Fig. 1 shows the dimensions and reinforcement details of the test specimen. Cross-section of all the specimens was 300 x 300 mm while the heights were 1000 mm and 850 mm for specimens of Series A and Series B respectively. Shear capacity of concrete, was evaluated by using Okamura-Higai equation as shown in Eq. 1 [13].

$$V_c = 0.2 f'_c^{1/3} (100 p_w)^{1/3} \left(\frac{1000}{d}\right)^{1/4} (0.75 + 1.4 \frac{d}{a}) b_w d \quad (1)$$

where,

$f'_c$  = compressive strength of concrete

$p_w$  = ratio of tensile longitudinal steel area to area of web concrete

$d$  = effective depth

$a$  = shear span

$b_w$  = web width of member

Design shear strength to flexural strength ratio of 0.8 was employed in the experiment. Identical longitudinal reinforcement details with 12 bars of 16 mm in diameter were provided in all the test specimens. Deformed bars with the diameter of 6 mm were used as lateral reinforcement. Table 1 shows the details of the test specimens, compressive strength of concrete, and quantity and yield strength of various kinds of reinforcing bars used in the specimen.

**Table-1 Details of the column specimens and material properties**

Sp. No.	a/d	Bond condition	Concrete strength $f_c'$ , MPa	Longitudinal bars		Lateral ties	
				$A_s$	$f_y$ , MPa	Size & spacing(mm)	$f_{wy}$ , MPa
A-1	3.0	Deformed bars	32.54	12-D16	380.18	D6@250	396.60
A-2		Unbonded bars	33.69	12-D16	380.18	D6@250	396.60
A-3		Round bars	34.12	12-φ16	324.06	D6@250	396.60
B-1	2.5	Deformed bars	28.76	12-D16	380.18	D6@150	396.60
B-2		Unbonded bars	30.47	12-D16	380.18	D6@150	396.60
B-3		Round bars	31.14	12-φ16	324.06	D6@150	396.60

### Method of Controlling Bond

In order to investigate the influence of bond, a total number of three bond conditions from the perfect bond to the perfect unbond were studied. Fig. 2 shows the methods used for bond control. In the specimens with perfect bond, normal deformed bars were used as longitudinal reinforcement. Poor bond condition was achieved by replacing deformed bars with round bars. The surface of the round bar in shear span was smoothened by using sand paper which was then followed by the application of grease before placing concrete.



(a) Poor Bond



(b) Perfect Unbond

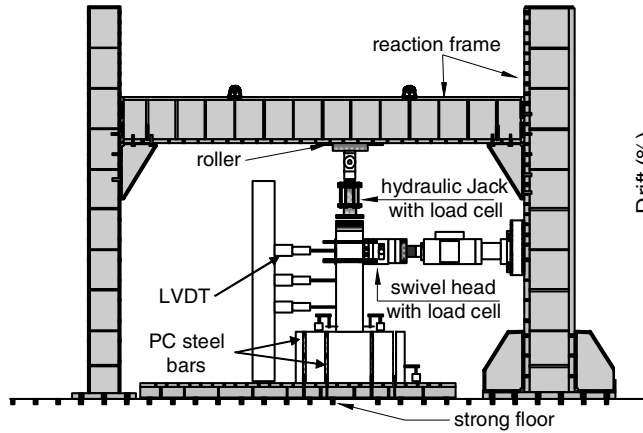
**Fig. 2: Method of controlling bond**

Complete unbonding of longitudinal bar was achieved by the use of spiral sheath. Before placing concrete, the desired length of longitudinal bar was inserted into the sheath. The location of the sheath was properly fixed and both ends of the sheath were made water tight by applying silicon gel. Sufficient development length was also provided to prevent undesirable anchorage failure.

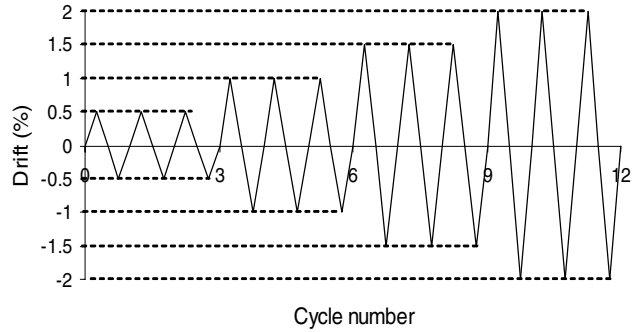
### Experimental Setup and Instrumentation

Fig. 3 shows the loading setup. The specimen was fixed on strong floor with prestressed rods. Reversed cyclic lateral load was applied at the designated loading point of the column by using an actuator. A

constant axial load of 90 kN was applied throughout the experiment in order to maintain the compressive axial stress of 1 MPa. Axial loading jack was designed to move freely with applied lateral displacement.



**Fig. 3: Experimental Setup**



**Fig. 4: Loading sequence**

Horizontal displacements at three different locations in the column, crack width at the column-footing joint and possible displacement and rotation of the specimen were measured by linear voltage displacement transducers (LVDTs) and strains in several locations of both longitudinal bars and lateral reinforcement were measured by using strain gages which were already fixed at the desired location before placing concrete.

### Reverse Cyclic Loading Test

The experimental procedure was identical for all the specimens. An axial load of 90 kN was first applied. Displacement controlled reversed cyclic loading was applied with the loading sequence as shown in Fig. 8, which consists of stepwise loading stages with each stage comprising of three number of cycles. Displacement amplitude of 0.5 % drift was applied in the first stage, where drift is defined as the ratio of lateral displacement to the effective height of the column. The displacement was then applied stepwise in an increment of 0.5 % drift until the specimen failed. Specimen is considered to have failed when the load carrying capacity degrades to 80% of its maximum value.

## RESULTS AND DISCUSSION

### Load-Displacement Curve

Load-displacement curves obtained from the experiment for both Series A and Series B are shown in Fig. 5. Specimen A-1 failed in shear before yielding of the longitudinal bars. Specimen A-2 with unbonded longitudinal bars completely avoided shear failure and eventually failed due to crushing and spalling of concrete followed by yielding of longitudinal bars. Specimen A-3 with rounds bars applied with grease coating showed better performance with significant improvement in ductility. Unlike A-1, Specimen B-1 failed in shear after the longitudinal bars yielded. With the change in the bond condition, similar to Series A, Series B also showed improvement in ductility and complete change in the failure mechanism from shear to flexure.

Pinching effect was clearly visible in the load displacement curves. This effect was attributed to the occurrence of wide diagonal shear crack with the load reversal in the case of Specimens A-1 and B-1. On the other hand, pinching in unbonded specimens was due to the occurrence of large flexural crack at column-footing joint.

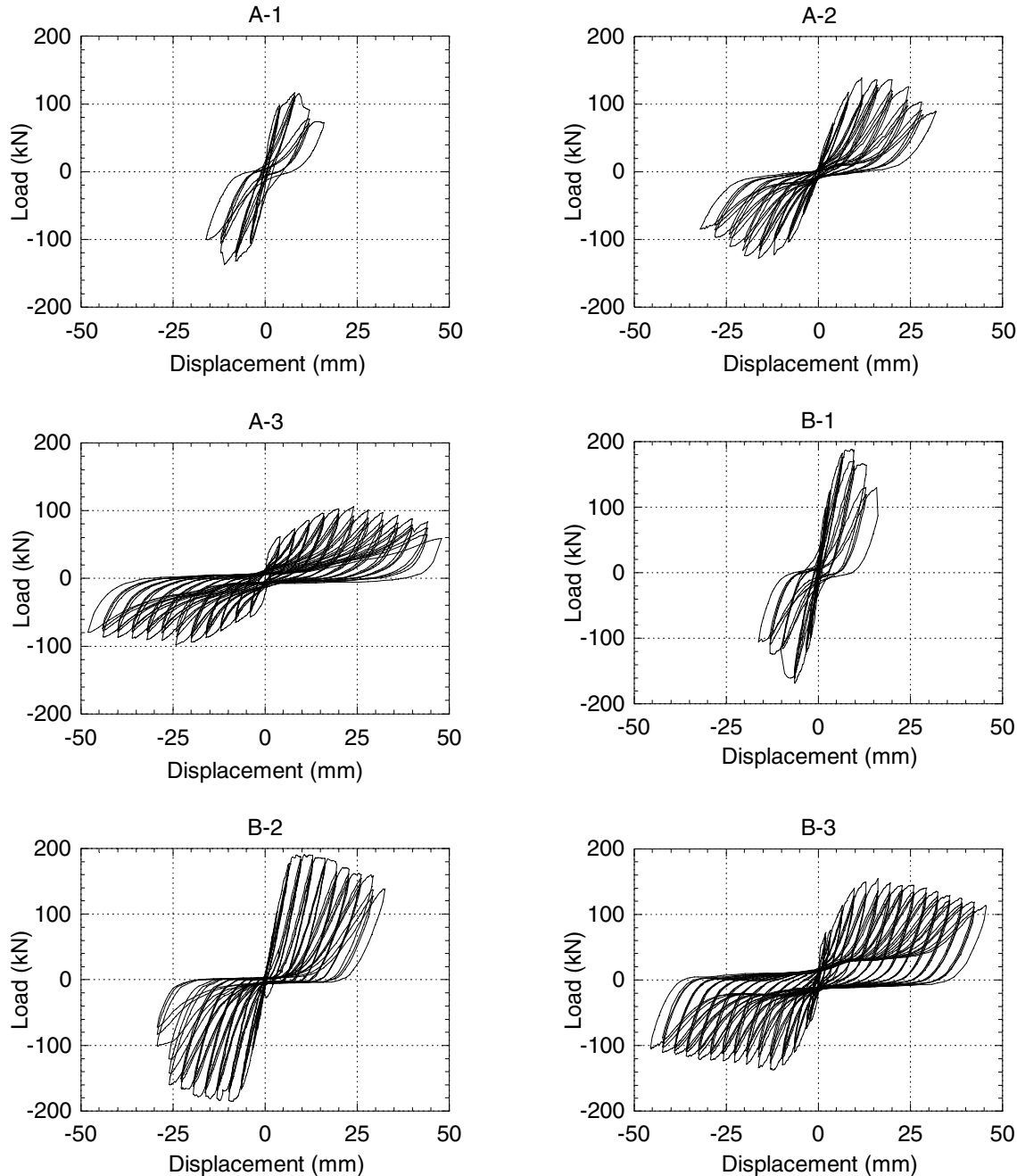


**Fig. 5: Load displacement curves of all tested specimens**

Comparison of load-displacement envelope curves in both the series are shown in Fig. 6. The envelope curves in Series A show that, by unbonding, the load carrying capacity of the specimen was increased due to the complete change in failure mechanism. It was also observed that there was a slight reduction of stiffness due to unbonding but remarkable increase in ductility. The best performing specimen was the one with round bar applied with grease. It showed flexural failure with more ductile behavior. The load carrying capacity of the specimen with round bars, however, appeared to reduce, which was attributed to the lower tensile strength of round bar than that of deformed bars. Series B also demonstrated the similar phenomena. Remarkable improvement in ductility was observed in the unbonded specimen with a very

little reduction in stiffness and delay in yielding. Seismic performance was further improved by replacing the ordinary longitudinal bars with round bars applied with grease.

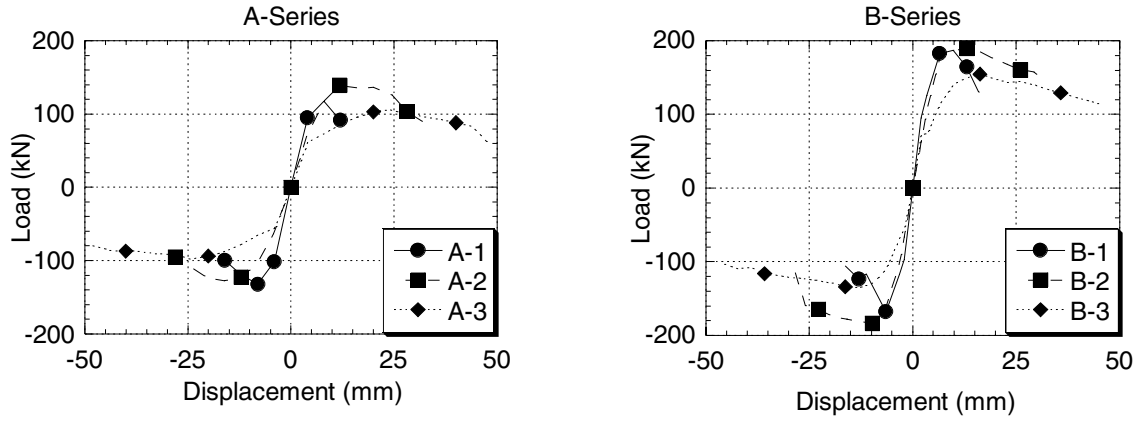


**Fig. 6: Load displacement envelope curves**

### Cracking Pattern

Fig. 7 shows the cracking pattern of all the specimens at failure. In the case of specimens A-1 and B-1, flexural cracks appeared at several locations on the specimen right from the first cycle. As the number of cycles increased, the crack furthered and then developed to diagonal shear crack. The final failure took place with the wide opening of diagonal crack resulted from the yielding of shear reinforcement. Load-displacement curve clearly shows a typical shear behavior. In case of specimens A-2 and B-2, the crack started from the column-footing joint first. With further loading, the crack width increased and propagated upwards. No single crack was formed at the sides of the specimen. The final failure was due to the crushing of concrete followed by yielding of the longitudinal bars.

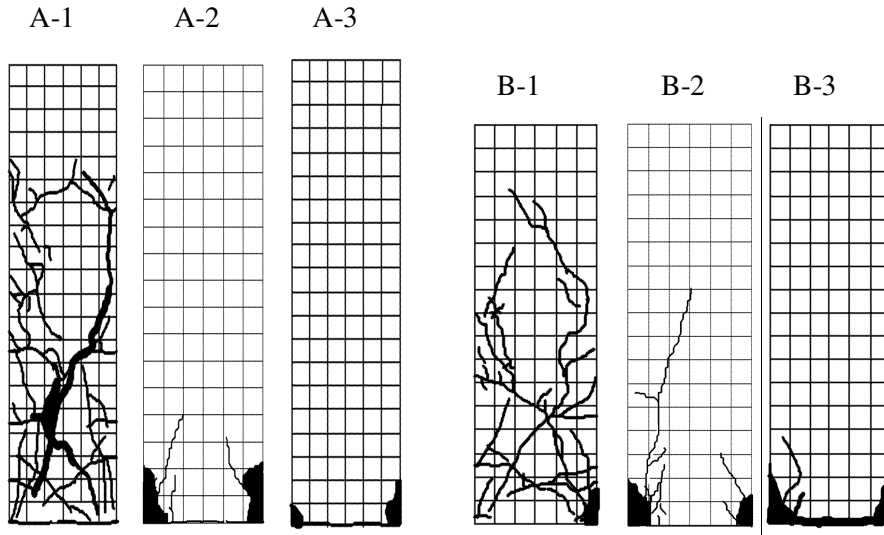


**Fig. 7: Cracking Pattern**

Specimens A-3 and B-3 also performed in similar manner as specimens A-2 and B-2. Damage was found to concentrate only at the column-footing joint. The final failure was due to crushing of concrete followed by yielding of the longitudinal bars.

## SEISMIC RESPONSE ANALYSIS

Though the improvement in shear resistance and ductility has been evident as a result of unbonding longitudinal bars, the major setback of this method is the low area of energy absorption and high residual deformation. To study the behavior of unbonded columns under earthquake loading, seismic response analysis has been carried out.

### Restoring Force Model

Among various restoring force models proposed by several researchers, Takeda Model has been the most commonly accepted one. In this study, a simplified Takeda Model with degrading stiffness and bilinear skeleton, as shown schematically in Fig. 8, is used for the ordinary reinforced concrete columns [14,15]. Load-displacement relation is considered to be linear elastic until the yielding point of column. Post yielding load carrying capacity is reduced with a slope of  $K_t$ , which is defined in Eq. 2a. Unloading stiffness, which depends on ductility is defined in Eq. 2b. Hysteretic laws for the inner loops of the model are in accordance with the model proposed by Takeda et al. [14].

$$K_t = 0.067 \frac{P_y}{Y_y} \quad (2a)$$

$$K_r = \frac{K}{\sqrt{\mu}} \quad (2b)$$

where,  $P_y$  is yield strength,  $Y_y$  is yield displacement,  $K$  is initial elastic stiffness,  $K_t$  is slope of reduction of load carrying capacity,  $K_r$  is unloading stiffness, and  $\mu$  is ductility, which is defined as the ratio of maximum displacement to yield displacement.

The model however does not show a good agreement with the load-displacement behavior of unbonded columns as sharp pinching occurs in the hysteresis loop due to the occurrence of wide crack at the column-footing joint. A large discrepancy can be observed when the model is compared with the experimental results as shown in Fig. 9.

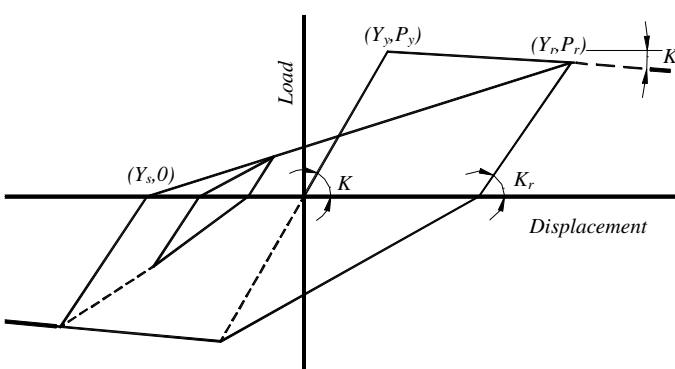


**Fig. 8: Schematic diagram of simplified Takeda Model**

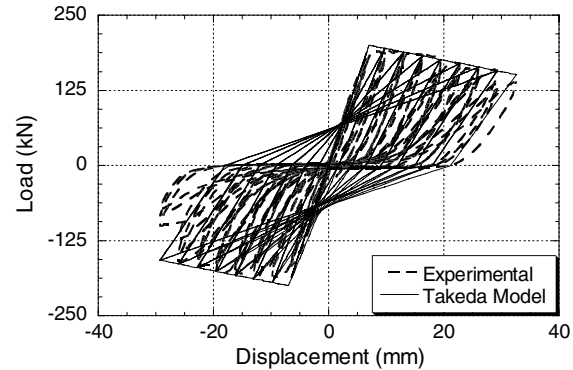


**Fig. 9: Comparison of Takeda Model with experimental result**

A new model is proposed with similar skeleton and inner loops while, the straight loading curve has been replaced by power curve as shown in Eq. 3. Degree of curvature of the loading curve, expressed by  $Z$ , is determined from the coordinate of highest turning point and the starting point of the loading curve as shown schematically in Fig. 10.

$$P = A(Y - Y_s)^Z \quad (3)$$

where,  $A = P_r / (Y_r - Y_s)^Z$ ,  $Z = 1.1 \frac{Y_r - Y_s}{Y_y}$ , and  $(P, Y)$  is the coordinate of the loading curve between  $(0, Y_s)$  and  $(P_r, Y_r)$ .

Apart from the modification in loading curve, unloading curve is also altered to incorporate the influence of unbonding longitudinal bars on residual displacement. Eq. 4 shows the stiffness of unloading curve for the proposed model.

$$K_r = \frac{K}{(\mu)^{1/4}} \quad (4)$$

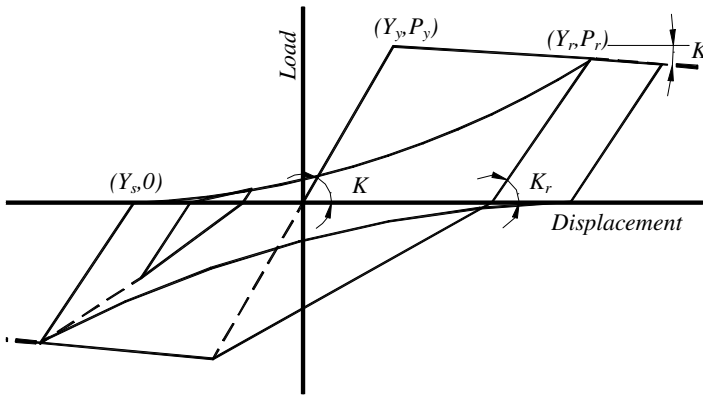


**Fig. 10: Schematic diagram of Proposed Model**

In the proposed model, the nature of loading curve can be controlled by a single parameter  $Z$ . If  $Z$  is defined to be unity, loading curve results to that of simplified Takeda model. Fig. 11 shows that the model has good agreement with the experimental results. In order to further verify the model, experimental cumulative energy absorption is compared with that of Takeda model and proposed model. Fig. 12 shows that the cumulative energy absorption of the proposed model agrees well with that obtained from experiment.

#### Nonlinear Response Analysis

The N-S wave of Kobe Earthquake with the maximum acceleration of 818 gal was used in the analysis. Time history of the acceleration is presented in Fig. 13. Response analysis was carried out for two different yielding ratios of 0.6 and 0.4. Yielding ratio is defined as the ratio of yield strength of the column to the gravity load carried by the column. Natural period of the structure, which depends on its height, is evaluated by using Eq. 5.

$$T = 2\pi \sqrt{\frac{m}{K}} \quad (5)$$

where,

$m$ = mass carried by column + 30% of column mass

$K$ =Initial elastic stiffness

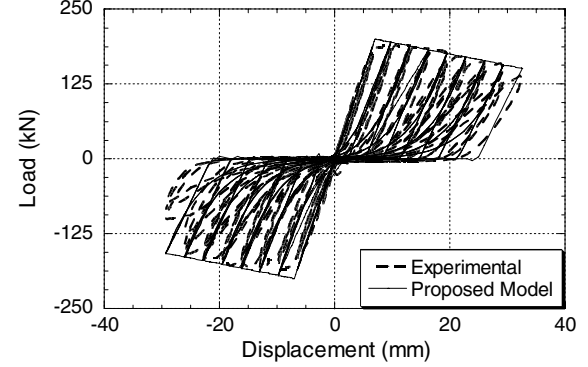


**Fig. 11: Comparison of Proposed Model with experimental result**

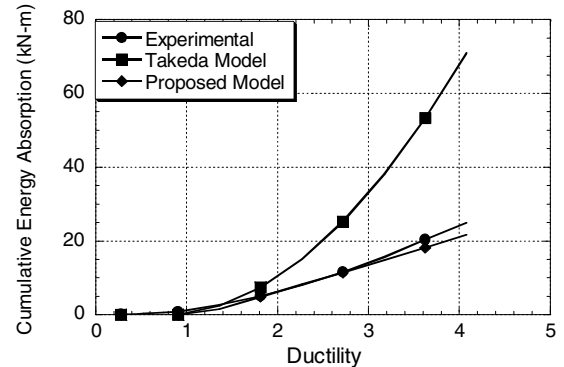


**Fig. 12: Comparison of cumulative energy absorption**

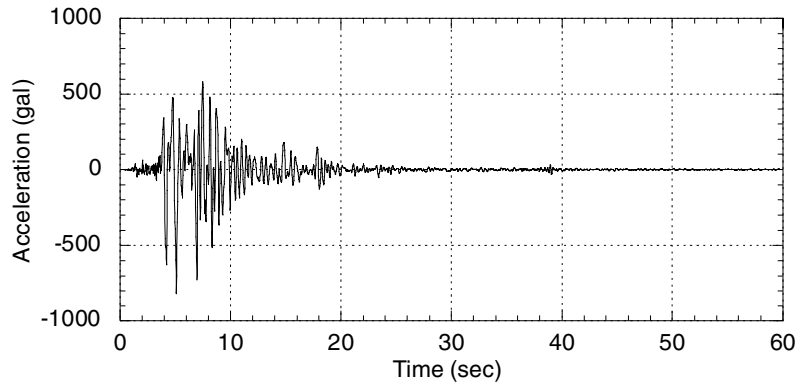


**Fig. 13: Kobe Earthquake wave (N-S) used in the analysis**

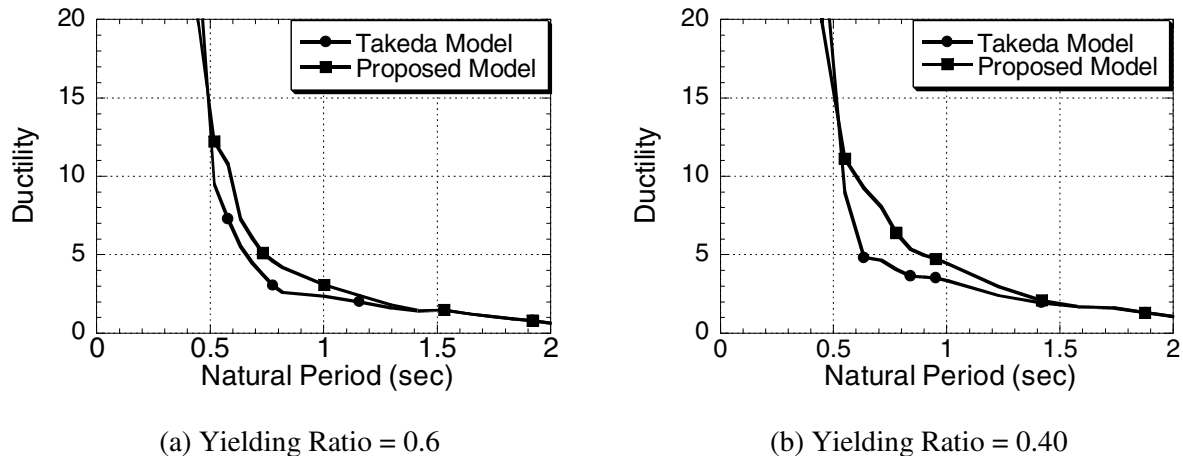


**Fig. 14: Response ductility Spectrum due to Kobe Earthquake**

Fig. 14 summarizes the results in terms of response ductility spectrum. Ductility is defined as the ratio of maximum displacement to the yield displacement. It can therefore be clearly observed that the unbonded columns show larger displacement response than that of ordinary RC column when the natural period of the column is in the range of 1~1.5 sec. This difference is attributed to the low area of energy absorption and hence the low damping of the unbonded columns. For the columns with the natural period larger than 1.5 sec, however, seismic response remains unaltered by unbonding longitudinal reinforcement.

## CONCLUSION

Reversed cyclic loading test was carried out on six RC columns with various bond conditions of longitudinal reinforcement. Nonlinear seismic response analysis was also carried out to compare the behavior of unbonded columns with the ordinary one. Based on this study the following conclusions can be drawn:

1. Unbonding of longitudinal bar can completely change failure mode at the ultimate state from shear to flexure and it remarkably increases the ductility.
2. Though both unbonding longitudinal bar and replacing deformed bars with greased round bars improve seismic behavior, the later technique yields better performance which is attributed to the poor bond of longitudinal bar embedded into the footing.

3. Unbonding of longitudinal bar, however, results in the lower area of energy absorption and larger residual deformation, which is responsible for larger seismic response especially when the frequency of the earthquake becomes closer to the natural frequency of the column.

## REFERENCES

1. ACI-ASCE Committee 445 on Shear and Torsion. "Recent approaches to shear design of structural concrete." Journal of Structural Engineering, Vol. 124, No. 12, pp. 1375-1417, 1998.
2. Hsu TTC. "Unified approach to shear analysis and design." Cement and Concrete Composites, Vol. 20, pp. 419-435, 1998.
3. Kawashima K. "Seismic design and retrofit of bridges." Proceeding of 12<sup>th</sup> World Congress on Earthquake Engineering, 2228, 2000.
4. Okamura H. "Japanese seismic design codes prior to Hyogoken-Nanbu Earthquake." Cement and Concrete Composites, Vol. 19, pp. 185-192, 1997.
5. Sezen H, Whittaker AS, Elwood KJ, Mosalam KM. "Performance of reinforced concrete buildings during the August 17, 1999 Kocaeli, Turkey Earthquake, and seismic design and construction practice in Turkey." Engineering Structures, 25, pp.103-114, 2003.
6. Design Specification for Highway Bridges, Part 5, Earthquake Resistant Design, Japan Roadways Association, 1996, 2002. (in Japanese)
7. Kani GNJ. "The riddle of shear failure and its solution." ACI Journal, Vol. 61, No. 4, pp. 441-467, 1964.
8. Ranasinghe K, Mutsuyoshi H, Ashraf M. "Effect of bond on shear behavior of RC and PC beams: experiments and FEM analysis." Proceedings of JCI, Vol.23, No. 3, pp.1057-1062, 2001.
9. Ranasinghe K, Mutsuyoshi H, Uchibori H. "Cyclic testing of reinforced concrete columns with unbonded reinforcement." Proceedings of JCI, Vol.24, No.2, pp.1141-1146, 2002.
10. Pandey GR, Mutsuyoshi H, Sugita K, and Uchibori H. "Mitigation of seismic damage of RC structures by controlling bond of reinforcement." Proceedings of the Japan Concrete Institute, Vol. 25, pp. 1441-1446, 2003.
11. Lees JM, Burgoyne CJ. "Experimental studies of influence of bond on flexural behavior of concrete beams pretensioned with aramid fiber reinforced plastics." ACI Structural Journal, Vol. 96, No. 3, pp.377-385, 1999.
12. Lees JM, Burgoyne CJ. "Analysis of concrete beams with partially bonded composite reinforcement." ACI Structural Journal, Vol. 97, No. 2, pp.252-258, 2000.
13. Okamura H, Higai T. "Proposed Design Equation for Shear Strength of Reinforced Concrete Beams without Web Reinforcement." Proc. of JSCE, No. 300, pp. 96-106, 1980.
14. Takeda T, Sozen MA, Nielsen NN. "Reinforced concrete response to simulated earthquakes." Journal of the Structural Division, proceedings of the American Society of Civil Engineers, Vol. 96, No. ST12, pp. 2557-2573, 1970.
15. Clough RW, Johnston WH. "Effect of stiffness degradation on earthquake ductility requirement." Proceedings of Japan Earthquake Engineering Symposium, Tokyo, Japan, pp. 195-198, 1966.